

Measurements of the LWA1 Station Beam and Antenna-based Gains using TBW Observations of RFI with Self-calibration

by J. F. Helmboldt

1 Introduction

To measure the station beam of the LWA1 phased array, ideally one would use an observation of a relatively isolated, bright source. Since the field of view of the LWA1 antennas is the entire observable sky and, at HF/VHF frequency, the sky is virtually filled with Galactic emission, this is rather difficult. Consequently, to date, efforts to measure the beam have been confined to observations of bright sources such as Cygnus A with the station correlated with the outlier antenna (see, e.g., *Ellingson*, 2011). This 300-m baseline is long enough to be insensitive to large angular-scale Galactic emission. However, having only one baseline makes the data somewhat noisy and special care has to be taken to mitigate the effects of other bright sources like Cassiopeia A (via fringe-filtering; again, see *Ellingson*, 2011).

An alternative method involves the usage of terrestrial sources. Usually regarded as radio frequency interference (RFI), transmitters such as local FM radio stations and ionospheric echoes of more distant transmitters can appear as extremely bright, isolated point sources. Since they are usually on the order of 100 km away or more, they can be imaged assuming the far-field approximation used for cosmic sources since LWA1 is quite compact by comparison (at least 1000 times smaller than the distance to the source). Such a source also offers the opportunity to use standard self-calibration techniques to solve for the complex, antenna-based gains for the station.

In this memo, I discuss preliminary results from imaging and performing self-calibration on TBW observations of an FM station (KUNM) and two bright, isolated echoes of analog TV stations at 55 MHz. The data show that by calibrating the array visibilities with the measured cable delays available from the LWA Software Library (LSL), the first sidelobes of the station beam are at -16 dB relative to the peak. This is only about 4 dB higher first sidelobes of the theoretical beam, which are at about -20 dB. After applying self-calibration, the beam is nearly indistinguishable from the theoretical beam, even when the gain solutions are derived using one bright echo and are applied to another. From a single TBW capture, the amplitudes of the gains determined from the FM station at 89.9 MHz and those at 55 MHz seem well-correlated. The phases also follow the expected trend for delay errors, that is, they scale with frequency.

2 Data and Analysis

The data used were produced from two archival TBW captures taken on 25 October 2011 at 00:02:31 and 00:11:18 UT. All images were produced using my own python-based software which performs a “brute-force” calculation of the intensity in the image plane from visibilities, taking non-coplanarity into account and relying on LSL to provided data for cable delays, gains, and antenna positions. The visibilities at 89.9, 55.25, and 55.26 MHz (see below) were

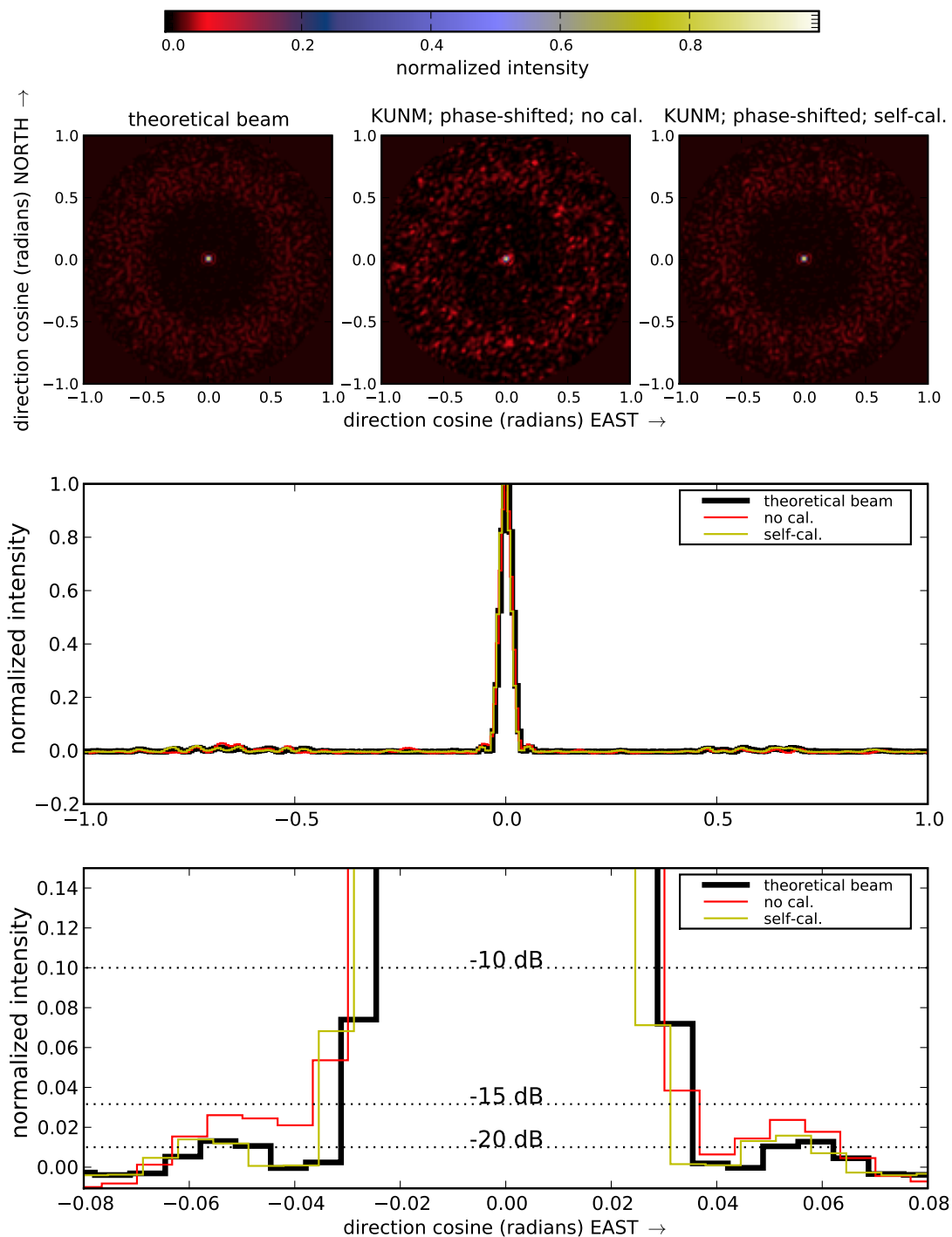


Figure 1: Upper: At 89.9 MHz the theoretical beam (left), a phase-shifted image of the KUNM transmitter (middle), and an image of the transmitter after self-calibration (right). Middle: East-west slices through the brightest pixels in the three images shown above. Lower: The same as the middle panel, but zoomed in to show the first sidelobes.

constructed from complex voltages generated via FFTs of the TBW signals. These visibilities were written out to FITS files readable by the CASA software package using templates kindly provided by J. Hartman. The template FITS files contained data for 253 out of 258 stands, excluding stands 9, 36, 148, 244, and 257 (the RTA antenna). For convenience, these stands were likewise excluded from this analysis so that the structure of the FITS files did not have to be altered from that of the template files.

2.1 FM Station

Because the signal from the FM station, KUNM, is spectrally relatively broad, a 95.7 kHz bandwidth was used to generate the complex voltages at 89.9 MHz (using an FFT with a window of 2048 TBW samples). I first applied corrections to this data to correct for unequal cable delays and losses according to the data available within LSL. I then applied an additional phase correction to put the KUNM signal in the middle of the field of view. I also computed the theoretical beam by simply setting all the visibilities to unity and re-running the imaging software. The beam and the image of the phase-shifted KUNM signal can be seen in the upper left and middle panels of Fig. 1. While they are similar, the sidelobes are clearly worse for the KUNM image. East-west slices through the peak pixels from both of these images are plotted in the middle and lower panels of Fig. 1 with the lower panel showing a “zoomed-in” version. From these, one can see that the first sidelobes of the theoretical beam are at about -20 dB, as expected. While the KUNM slice clearly has higher sidelobes, they are only at about -16 dB, significantly lower than has been found with other techniques (again, see e.g. *Ellingson*, 2011).

Next, the completely uncalibrated KUNM visibilities were read into CASA and an amplitude and phase self-calibration was run on them assuming a point-source at the origin. During this calibration, 27 of the stands were flagged as having bad or no solutions in both polarizations. These are listed in Table 1 both by their stand names and by the stand indices (0-259) as they are ordered within LSL. This calibration was applied to the data, written out to a FITS file, and imaged with my software within python. The resulting image is shown in the upper right panel of Fig. 1. There is no noticeable difference between it and the theoretical beam. East-west slices from this image are also plotted in the middle and lower panels of Fig. 1. They show that while this image and the theoretical beam peak at slightly different pixel values, their sidelobes appear nearly identical.

2.2 TV Stations

As a sanity check, I sought to take self-calibration-determined antenna gains derived from one source and apply them to another source at a similar frequency as a first-order check of the reliability of the gains. For this, I used a relatively unique occurrence of two relatively bright echoes of two different analog TV broadcasts at similar but different frequencies. The echoes are from the video carriers for channel 2 (55.25 MHz) and channel 2⁺ (55.26 MHz) and were observed in the second of the two TBW captures mentioned above. These signals are spectrally quite narrow and to isolate them, I made complex voltages with a 186.9 Hz bandwidth (using an FFT with a window of 2²⁰ TBW samples). Images of both echoes can

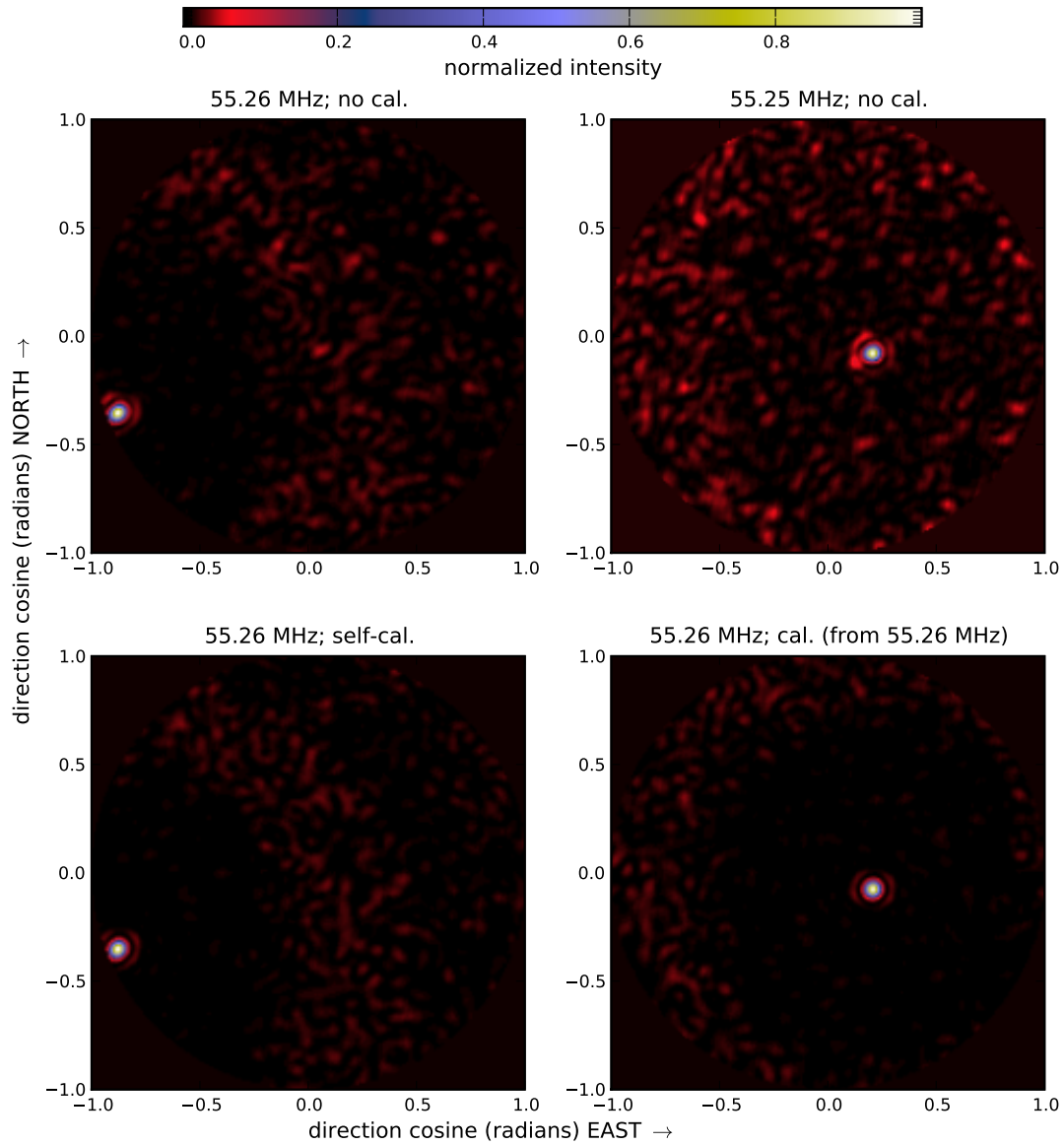


Figure 2: Images of echoes at 55.26 MHz (left) and 55.25 MHz (right) before (upper) and after (lower) applying gain corrections derived from performing self-calibration with the 55.26 MHz echo.

be seen in the upper panels of Fig. 2 made with only the cable delay and loss corrections applied to the visibilities.

Since the 55.26 MHz echo was brighter, the data for it were read into CASA first. Next, an image was made within CASA with very light cleaning to establish a model for self-calibration (note, it does not appear to be possible to specify a point source at a particular location within the CASA routine `gaincal` as it is within the AIPS task `CALIB`). Next, amplitude and phase self-calibration was performed and the gain corrections were applied to both the 55.26 and 55.25 MHz data. Note that the same 27 antennas were flagged again during this process as were flagged by self-calibration using KUNM with a different TBW capture (see §2.1 and Table 1). Images were then made of the calibrated data and can be seen in the lower panels of Fig. 2. From these, one can see that the 55.26 MHz calibration considerably improves the sidelobes for both images. This is even more apparent in east-west slices through the peak pixels of both echoes shown in Fig. 3 along with the theoretical beam (note, the left sidelobes of the 55.26 MHz echo are missing because it is near the horizon). As with KUNM, applying the self-calibration-determined gains has brought the level of the first sidelobes down to that of the theoretical beam, even when derived using one source and applied to another.

2.3 Comparing Both

TBW data affords the unique opportunity not only to self-calibrate on bright transmitters, but also to do so simultaneously at multiple frequencies. Thus, we can see how the derived antenna gains change with frequency, which can reveal much about phase errors within the system. To this end, I self-calibrated on KUNM using the second TBW capture, this time starting with a clean model generated by imaging the transmitter within CASA. This was done so that the resulting gains could be directly compared to those derived from the bright 55.26 MHz echo (see §2.2). In Fig. 4, I have plotted the amplitude and phase of the 55.26 MHz gains versus those of the 89.9 MHz gains, separately for each polarization. While there is much scatter, the gain amplitudes are clearly correlated between the two frequencies. The scatter appears somewhat worse in Y-polarization. With a few exceptions, the phases seem to follow the trend expected for basic delay errors, that is, they scale with frequency.

The fact that the phase corrections seem to scale with frequency seems to bode well for the utility of these types of derived gains. In other words, it may be possible to calibrate on a very strong transmitter like KUNM, and then apply the gain corrections at other frequencies by simply scaling the phase components of the gains. I tried doing just that to the 55.25 MHz data of the bright channel 2 echo. In Fig 5, I show two images of the echo, one calibrated with the 55.26 MHz gains and one with the 89.9 MHz gains with the phases scaled by 55.25/89.9. The theoretical beam is also shown again for comparison. While the 55.26 MHz gains clearly do a better job of minimizing far-out sidelobes, east-west slices through the brightest pixels of all three images shown reveal that the 89.9 MHz gains did reduce the level of the first sidelobes down to that of the theoretical beam.

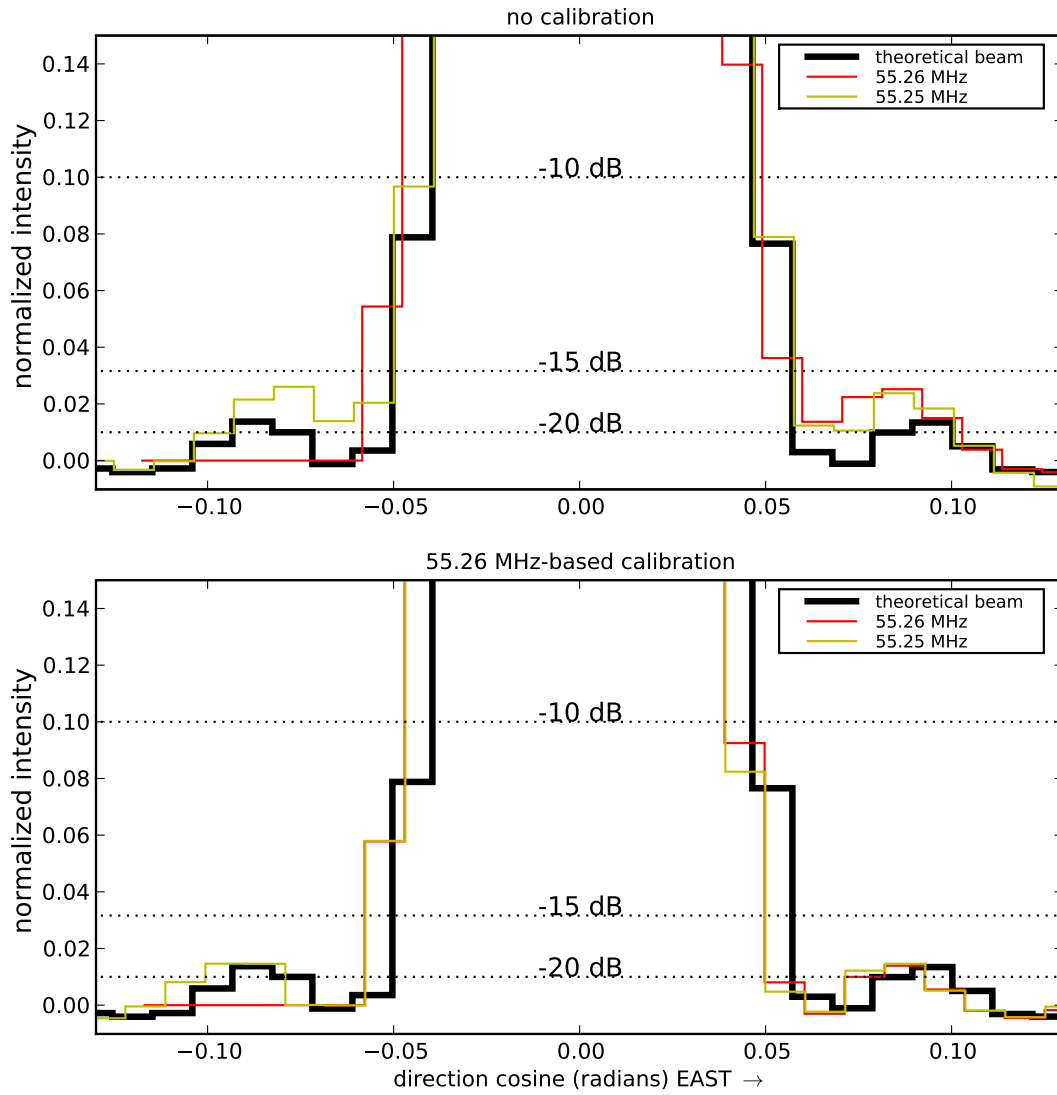


Figure 3: East-west slices through the brightest pixels in the images shown in Fig. 2 as well as the theoretical beam before (upper) and after (lower) self-calibration.

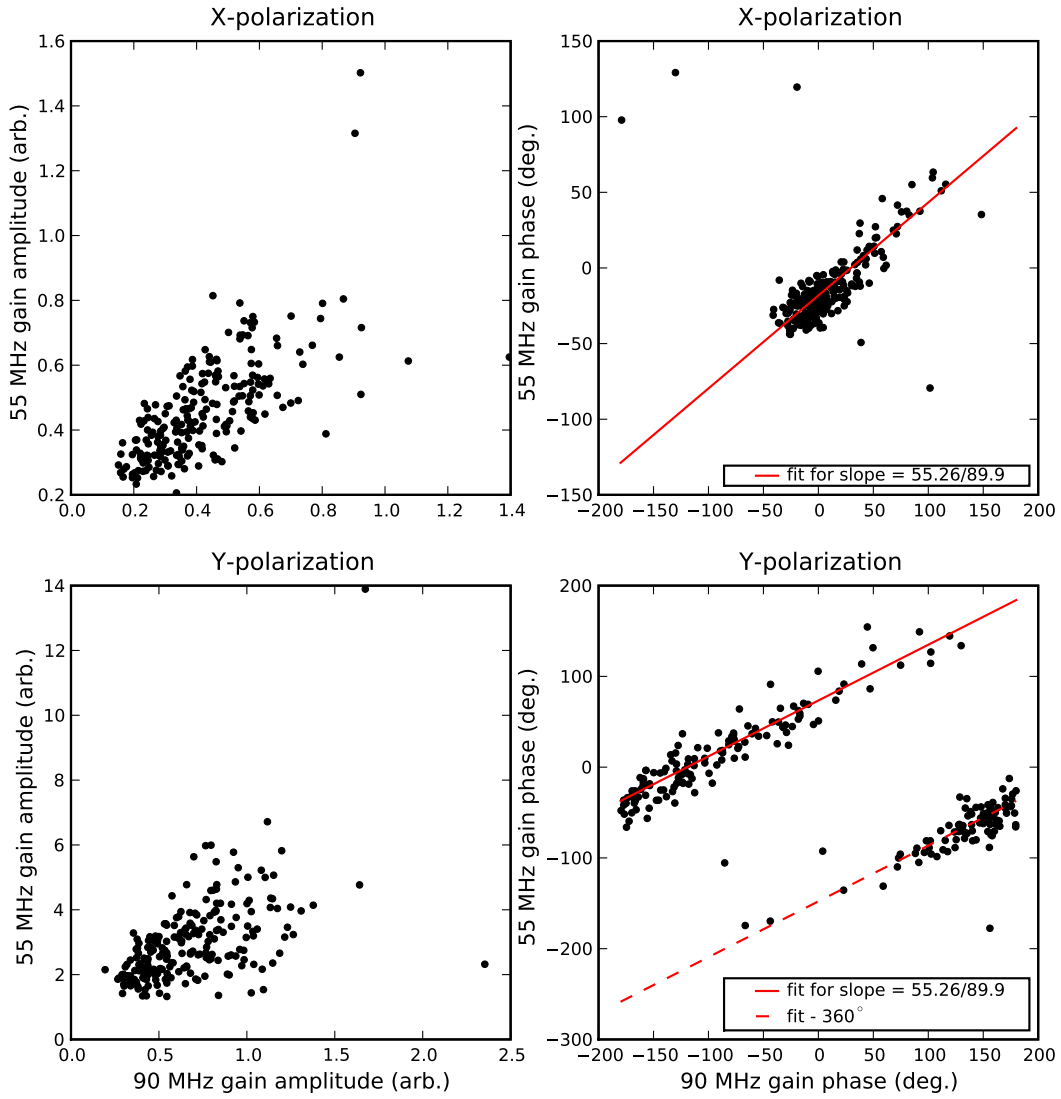


Figure 4: The amplitude (left) and phase (right) of the 55.26 MHz gains versus those determined at 89.9 MHz for the X (upper) and Y (lower) polarizations. In the right panels, the red lines show the expected relationship if the phases simply scale with frequency (i.e., a line with a slope of 55.26/89.9).

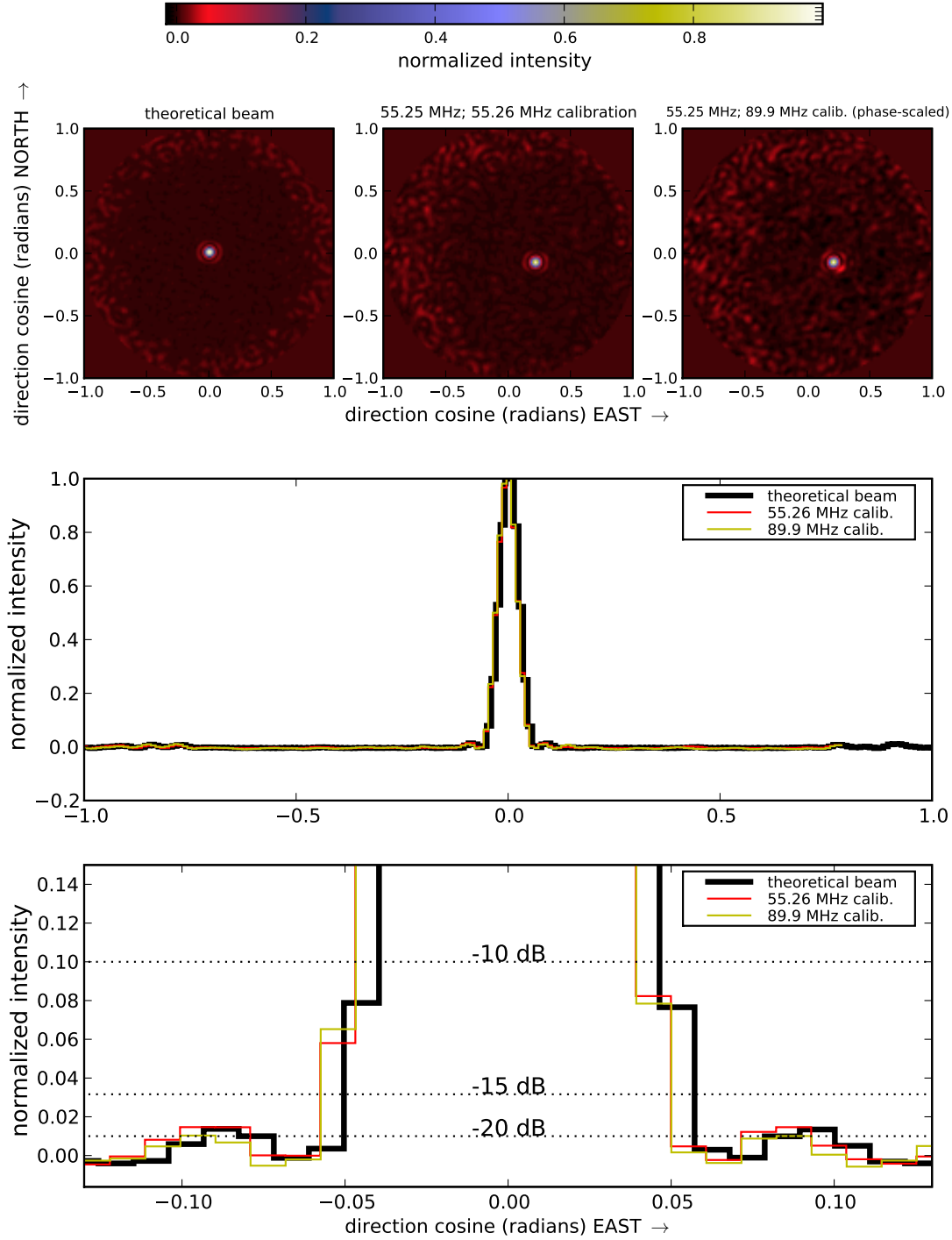


Figure 5: Upper: The theoretical 55.25 MHz beam (left), the 55.25 MHz echo calibrated with the 55.26 MHz gains (middle) and the same calibrate with the 89.9 MHz gains. East-west slices through the peak pixels of these three images are shown in the lower two panels.

3 Conclusions

The results of this study are generally encouraging. First, despite previous results, they show that the station beam has relatively reasonable sidelobe levels, -16 dB below the peak. Additionally, it appears to be possible to correct for the gain errors that give rise to these higher sidelobes via applications of standard self-calibration techniques, bringing the sidelobe levels down to about -20 dB. Note that in both cases, relatively narrow bandwidths were used, implying that the measured sidelobes are relatively unaffected by bandwidth smearing. This is especially true for the TV signal echoes where the bandwidth used was < 200 Hz. Thus, the results seem to point toward errors in the estimates for delays and losses within the system rather than more complicated, second-order effects like mutual coupling. However, by comparing one polarization to another for a single frequency, one can see that errors that would effect both polarizations equally (e.g., errors in the measured cable lengths) cannot account for these gain errors. One can see this in Fig. 6 where I have plotted the amplitude and phases of the 89.9 MHz gains for the Y polarization versus those for the X polarization. While the amplitudes are roughly correlated, the phases are not. The phase errors also seem to be much larger in the Y polarization, leading to a much poorer beam performance in Y polarization (see <http://lwa1.freeforums.org/mutual-coupling-worse-in-y-polarization-t19.html> for an example). Despite this, it appears that the gains determined from one frequency are easily scaleable to other frequencies, implying a possible method for calibrating the station.

In the future, I am planning on performing the KUNM-based analysis on many TBW captures to examine how stable the antenna-based gains are over time. I am also planning to use new TBN data at 55.25 MHz as well as at 10 and 15 MHz with the same methods described here to determine the TBN-based beam to assess whether or not the TBN filters cause any significant additional gain errors.

References

Ellingson, S. W. (2011), "Fun with TBN," Long Wavelength Array Memo 184, September 2011

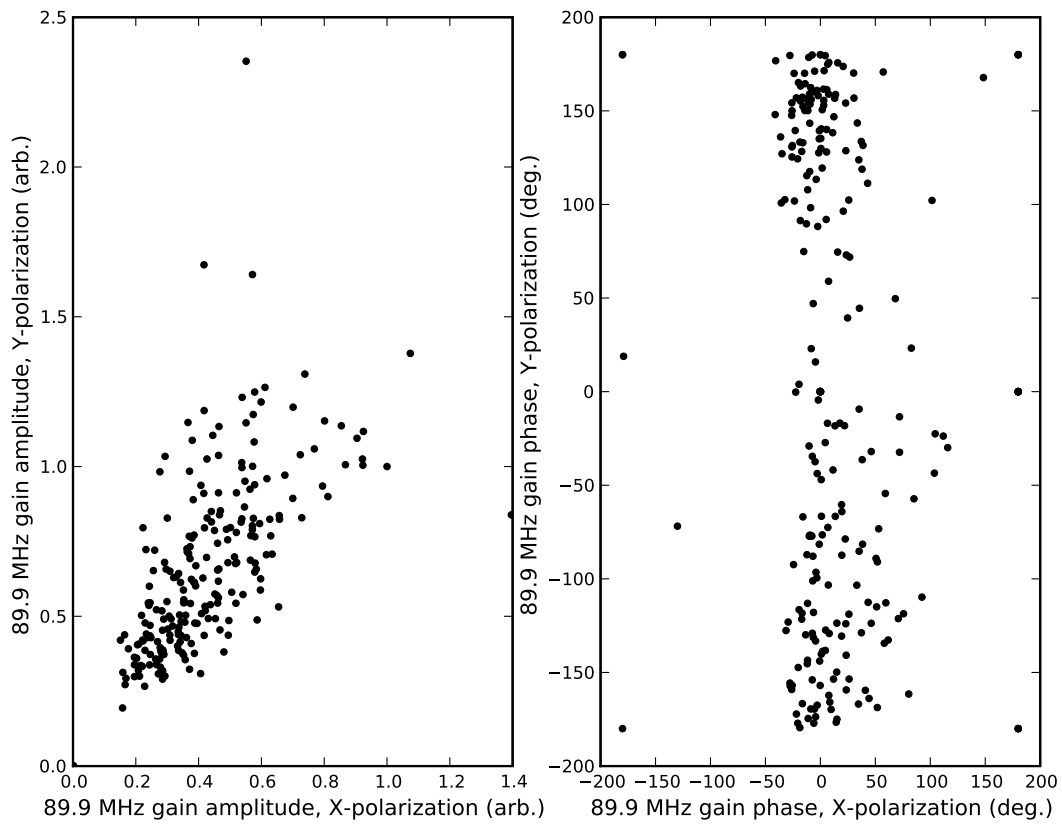


Figure 6: The amplitude (left) and phase (right) of the 89.9 MHz gains from the Y polarization versus those from the X polarization.

Table 1: Flagged Stands

LSL Stand Index	Stand Name
9	STD097
21	STD085
26	STD203
36	STD074
37	STD037
57	STD031
70	STD095
81	STD225
89	STD153
100	STD187
102	STD123
112	STD192
128	STD181
143	STD114
165	STD232
172	STD024
184	STD047
187	STD246
190	STD013
192	STD066
193	STD058
196	STD098
198	STD022
209	STD096
231	STD034
245	STD124
247	STD184